Mechanical Design and Optimization of a Microsurgical Robot

M. Miroir[1 2], J. Szewczyk[1], Y. Nguyen[3], S. Mazalaigue[2], A. Bozorg Grayeli[3], O. Sterkers[3]
[1] Université Pierre et Marie Curie-Paris 6, FRE-2507
Institut des Systèmes Intelligents et Robotique (ISIR), Paris, France
[2] Collin SA, Bagneux, France
[3] Inserm, Unit-M 867, Paris; AP-HP Hôpital Beaujon, Service d'ORL, Clichy; Université Denis-Diderot, France
e-mail: miroir@isir.fr

ABSTRACT- The tele-operated system with three arms for the microsurgery of the middle ear is composed of an operator console from where the surgeon tele-operates three robotized arms that hold surgery tools with a high level of accuracy. The main difference between these micromanipulators and the conventional minimal-invasive surgery robots is the increased field of vision capacity to carry out complex operational gestures without using dextral tool with intra-body mobility. The method used to design the micromanipulator tool holder is described. A first task consists of analyzing functional specifications. The next step is to define and select a kinematic structure adapted to the task. Finally, a dimensional optimization is carried out by using Pareto front method.

KEYWORDS: Surgery, Manipulators, Mechanism Design, Kinematics.

INTRODUCTION

For more than ten years, important developments in robotized minimal invasive surgery have been carried out in the fields of laparoscopy [1] or cardiac surgery [2]. The goal is to improve the precision, the safety of the gesture and the comfort of the surgeon.

In contrary, the robotic assistance to microsurgery is a recent research domain with many potential applications in the fields of cerebral [3], ophthalmologic [4] or ENT [5] [6] surgery. In this case, the design of a robotic assistance system has to face with specific problems, and nowadays no robotized device dedicated to the microsurgery is used in a clinical context.

Our main objective is thus to develop a robotized system for the microsurgery and particularly the middle ear surgery (Fig. 1). Different robotic systems have already been developed and dedicated to this surgery

[7], [8] and [9]. However, these systems do not fully satisfy all the task requirements and in particular the problems of overall size limitation and fabrication costs minimization. Our objective is thus to design a robot for the microsurgery which is:

- Small enough to allow the use of three systems at the same time without cluttering the environment or modifying the ordinary operating layout.
- Dexterous enough to avoid using any intracorporal mobility which leads to significant additional costs in terms of development, fabrication and maintenance.

Our approach will take into account all the technical constraints related to this particular kind of intervention. Moreover, economic and technological requirements inherent to every industrial product will be considered.

In this paper, we first describe the concerned surgical application and characterize the tasks devoted to the controlled device. The choice and the optimal dimensioning of a kinematic structure and of the actuators are then presented. Finally, geometrical parameters of the chosen structure are optimized in regards to the specifications.

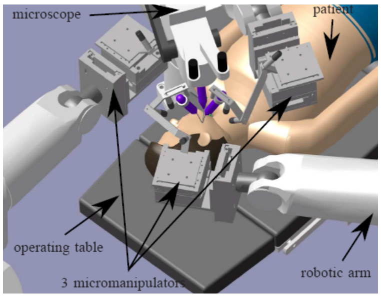

Fig. 1: Overview of a possible assistance robot for the middle ear surgical intervention

DESIGN SPECIFICATIONS AND EXPECTED PERFORMANCES

The presented system should be able to perform a surgical intervention in the middle ear. In most cases, the considered intervention uses the auditory canal with incision of the tympanic membrane as insertion path for the instrument [10], [11]. The patient's head is oriented on one side and immobilized. The surgeon can observe the operation area only through a microscope placed above the auditory canal at a maximum height of 300 mm. The tools (three of them can be used during the intervention at the same time) are introduced into the patient's ear through a funnel-shape speculum. Thus, the developed system should include three independent and simultaneously-controlled mandatory micromanipulators, each dedicated to the manipulation of one tool. These three micromanipulators will be identical, based on the same kinematic and dimension. The surgeon tele-operates the unit using a remote device.

In order to quantitatively specify the task, different measurements were taken. First of all, the manipulator workspace was identified by measuring the anatomy of the ear for ten different patients by means of X-rays and the navigation system *Digipointeur®* [12]. Fig. 2(a) presents a geometrical modeling of this workspace. It includes:

- In terms of reachable points: A volume made up of the external auditory canal, and the visible part of the case of tympanum,
- In terms of reachable orientations: All the achievable orientations considering a rectilinear tool introduced into this volume.

The interaction forces between the tool and the bones were measured using an experimental setup (Fig. 2(b)) including an *ATI nano43* 6-axis gauge force/torque sensor [13]. We found that the forces applied at the tip of the tool by the surgeon never exceed 3 N. Besides, our clinical partners consider as acceptable a motion resolution not exceeding 5 µm in translation and 1 ° in rotation. Finally, a geometrical modeling of the environment was proposed (Fig. 2(c)) which will be useful to evaluate the obstacle avoidance and vision preservation capabilities of the overall system.

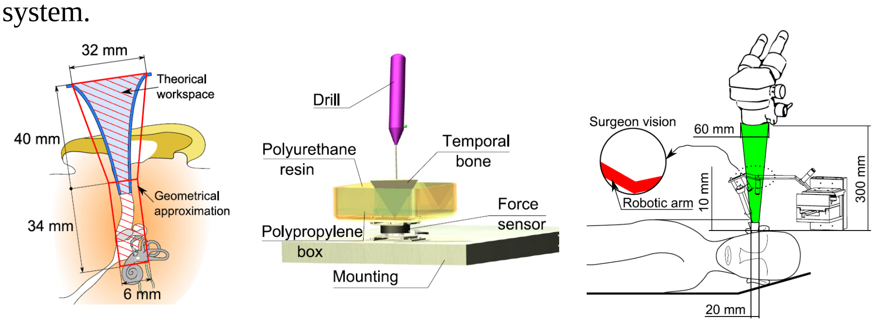

(a) *(b)* *(c)*

Fig. 2: From left to right, (a) geometrical approximation of the workspace, (b) experimental setup for measuring the forces, and (c) a global view of the intervention environment

TOPOLOGICAL STRUCTURES

Fig. 3 shows four candidates of possible kinematic structures. These structures are kinematically non-redundant in order to minimize the complexity and costs. All these structures are mounted on Cartesian “cross tables” in order to decouple translations from rotations of the tool. Moreover, the large displacements along the speculum axis can be entirely supported by the Z-axis of the cross table. In the same way, the four structures have a final rotoid joint devoted to perform large rotations around the tool axis.

The kinematics of Fig. 3(a) is a classical serial structure finished by a convergent wrist with orthogonal axes. This kind of structure is relatively simple to design and to control. However, it presents the disadvantage of a rotation centre outside the specified workspace. Indeed, rotating around the tip of the tool would imply in this case very large displacements at the X and Y axis of the cross table. Assuming a tool having a length of 15 cm for example, commanding a +/-20 ° rotation around the tip of the tool in any plane including the workspace principal axis would lead to a more than 10 cm horizontal displacement of the cross table.

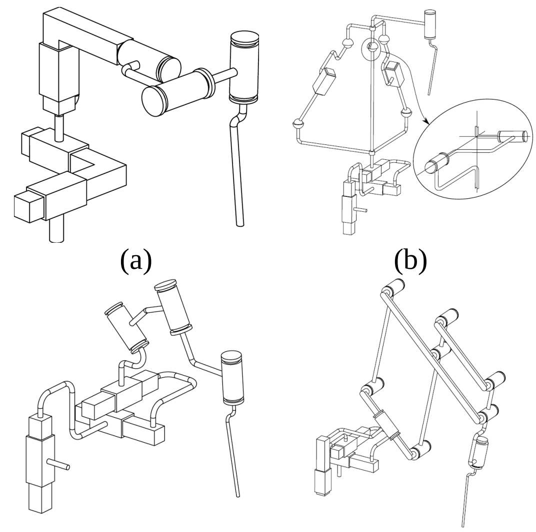

(a) (b) (c) (d)

Fig. 3: Kinematic candidates: (a) 6 dof series, (b) 6 dof mixed, (c) 6 dof series with offset rotation centre (orc), (d) 6 dof Evans with orc

The kinematics of Fig. 3(b) has a standard parallel platform well suited for achieving linear and angular displacements with a high accuracy. However, the overall size, weight and complexity are undesirable for the targeted application and it does not have a rotation centre in the workspace either.

The kinematics of Fig. 3(c) has a rotation centre located at the intersection of the three last rotations axis. A clever choice of these axes allows the centre of rotation to coincide perfectly with the end of the handled tool.

The kinematics of Fig. 3(d) also carries out an offset rotation centre by means of a motorized parallelogram (mechanism of Evans). Moreover, it allows an increased rigidity and thereby a higher accuracy. However, this kinematics is complex compared to the previous one and the height of the structure is not compatible with the microscope observation.

In conclusion of this qualitative analysis of kinematics candidates, the design of the micromanipulators will be based on the structure presented on the Fig. 3(c).

Fig. 4 shows the selected kinematic structure with its motorized joints. The actuators of the cross table are *Owis* linear motors which provide an impressive stroke/size ratio. The first two actuators have a stroke of 25 mm and the third one has 100 mm. The rotation actuators used for the three rotoid links are *Faulhaber* coreless DC motors selected by their good weight/power ratio.

These actuators guarantee a sufficient displacement resolution at the tip of the tool in regard to the specifications. Indeed, if d is the axial resolution of the cross table motors, we know that the resolution in linear displacement at the tip of the tool d_{max} is such that $d_{max} < \sqrt{3}d$. If $d = 2$ µm (as specified by the manufacturer) then $d_{max} = 3{,}5$ µm which is lower than the desired resolution $d_{des} = 5$ µm. On the other hand, if q is the angular resolution of the chosen rotation actuators, we know that the resolution in angular displacement of the tool q_{max} will never be larger than $3q$. Then, if $q = 0{,}2\text{x}10^{-3}$ ° (as specified by the manufacturer) we will have $q_{max} = 0{,}6\text{x}10^{-3}$ ° which is much lower than $q_{des} = 1°$.

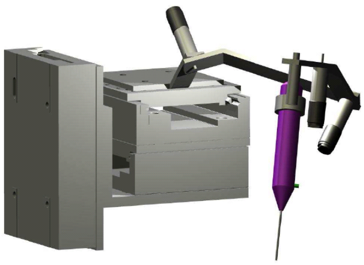

Fig. 4: Equipped kinematics

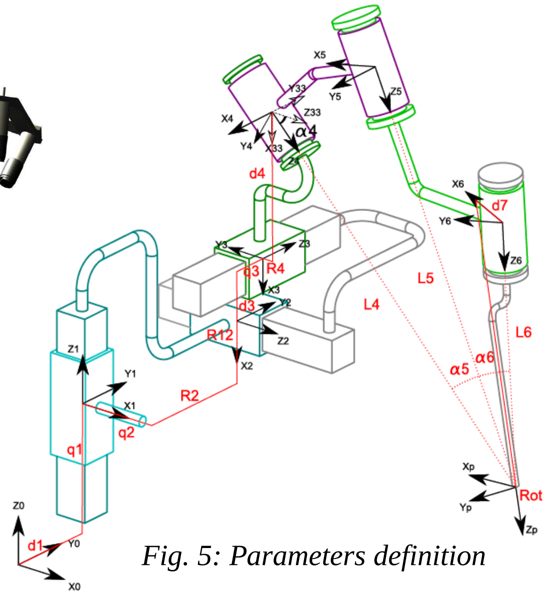

Fig. 5: Parameters definition

GEOMETRICAL OPTIMIZATION

Fig. 5 shows the joint parameters of the kinematic structure. Five parameters relate to the position of the cross table and are imposed by the dimensions of the chosen linear motors. The other six parameters (Table 1) relate to the position of the three rotoid joints and the relevant dimensions of the manipulator.

	$\alpha 4$	$L5$	$\alpha 5$	$\alpha 6$	$d7$	$L6$
mini values	25 °	90*mm*	25 °	15 °	5*mm*	130*mm*
maxi values	55 °	140*mm*	60 °	60 °	25*mm*	180*mm*
pitch	5 °	10*mm*	5 °	5 °	5*mm*	10*mm*

Table 1: Parameters values related to pivots and dimensions

The values of these remaining geometrical parameters were optimized with respect to the requirements that have not yet been taken into account at this stage:

- Ability to apply the desired forces,
- Distance to the obstacles,
- Occlusion of the field of vision.

The performances of the 90472 manipulators corresponding to the 90472 sets of parameters indicated in Table 1 were evaluated using a numerical simulation. This simulation consists of calculating all the successive configurations reached by the manipulator when the tool performs a specific 6D trajectory. This trajectory includes an approach path from an initial reference position and an operative path representative of the workspace in terms of angular and linear displacements. During this trajectory, the upper surface of the cylinder is swept by the end of the tool (see Fig. 6) in 30 steps: 17 for the circle and 13 for the spiral. For each step, the capacity of the robot to produce the maximum slopes of its tool is evaluated in 9 steps. Finally, for each configuration, the capacity of the manipulator to perform a rotation of the tool along its own axis is evaluated with 9 steps.

As rotation and translations are decoupled, it must be pointed out that the accessibility to the other points of the cylinder does not need to be evaluated. Remarkably, the vertical axis of the robot has a sufficient stroke in comparison with the depth of the workspace. The trajectory thus generated is made up of 2433 configurations ([[17+13]x9x9]+3) including 3 for the approach of the tool. For each reached configuration, the simulation computes:

- The forces that the manipulator can apply at the tip of the tool,
- The smallest distance robot/environment,

• The field of vision percentage of the microscope not intercepted by the arm of the robot,

• The stroke imposed to the joint actuators.

Finally, only 4063 candidate manipulators are able to perform the entire trajectory without contacting the environment or going beyond their joints limits and to produce at each step of the trajectory the required tip of the tool forces without exceeding their motors capacities.

Each retained manipulator is represented on Fig. 7 by a point positioned according to its scores in terms of smallest distance to the environment during the trajectory and average percentage of non-obstructed vision.

A Pareto's front made up of eleven non-lower solutions [14], [15] can be highlighted on this graph. This Pareto's front has the characteristics of nearly vertical graphs, all the scores in vision lying between 90% and 93.5%. Logically, we selected the manipulator presenting the best score in terms of distance to the environment. Table *2* presents the geometrical parameters of the eleven non-lower solutions. The last row corresponds to

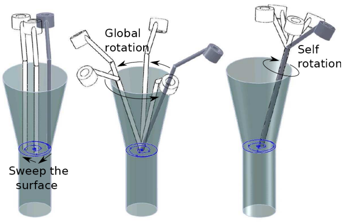

Fig. 6: Tool representative trajectory used for the optimization process

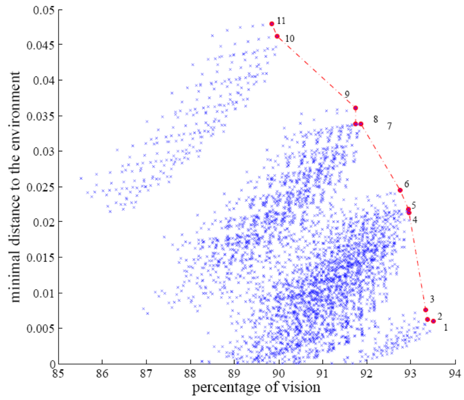

Fig. 7: Acceptable configurations plotted

α4 (°)	*L*5 (mm)	α5 (°)	α6 (°)	*d*7 (mm)	*L*6 (mm)	Vision (%)	Distance (mm)
30	140	60	50	10	180	93.5	6
50	140	50	50	10	180	93.5	6.2
40	140	40	50	10	180	93.3	7.5
40	140	55	45	5	180	92.9	21.3
50	140	45	45	5	180	92.9	21.7
50	140	40	45	5	180	92.7	24.4
35	140	55	40	5	180	91.8	33.8
50	140	40	40	5	180	91.7	33.8
55	140	40	40	5	180	91.7	36.1
35	140	55	35	5	180	89.9	46.2
55	140	35	35	5	180	89.8	47.9

Table 2: End values for the eleven possible solutions

the selected configuration.

CONCLUSION AND FUTURE WORK

This paper presents a detailed approach for the design of a robotic system in the field of microsurgery. It led to a multi-criteria optimization problem resolution in which constraints such as precision and compactness were taken into account. The implemented optimization method is based on a systematic exploration of the parameters domain and a *MatLab* routine for the constraint evaluations. At this stage, the robot is entirely defined in its geometry and motorization. The robot structure we propose has a compact geometry and allows performing any 6 dof displacements of the tip of the tool into the workspace of the external and the middle ear. Moreover, prototypying this structure will be relatively simple noting that it does not include any miniature intracorporal mobility. Future work concerns realization and performances test via coworking with the clinical partners.

REFERENCES

[1] Guy-Bernard Cadière, and al, "Feasibility of Robotic Laparoscopic Surgery", *In WORLD Journal of SURGERY*, Vol. 25, No. 11, pages 1467–1477, November 2001.

[2] Nabil Zemiti and al "Mechatronic Design of a New Robot for Force Control in Minimally Invasive Surgery", *IEEE/ASME Transactions on Mechatronics*, vol 12(2), april 2007,pp 143-153.

[3] P. Di Donato and al "La neuronavigation : principe et intérêt", ITBM-RBM 2000, 21:70-7.

[4] Natalie Smith-Guerin, "Contribution à l'aide robotisée au geste chirurgical ; nouvelle approche en ophtalmologie", PhD thesis, Laboratoire d'Automatique Industrielle de l'INSA de Lyon, 2000.

[5] Russell H. Taylor and al "A Steady-Hand Robotic System for Microsurgical Augmentation", *In MIC- CAI '99 : Proceedings of the Second International Conference on Medical Image Computing and Computer-Assisted Intervention*, pages 1031–1041, London, UK, 1999. Springer-Verlag.

[6] Daniel L. Rothbaum and al "Robot-Assisted Stapedotomy Micropick Fenestration of the Stapes Footplate", *Otolaryngology Head & Neck Surgery Journal*, vol. 127(5), 2002, pp 417-426.

[7] Peter J. Berkelman and al "Performance Evaluation of a Cooperative Manipulation Microsurgical Assistant Robot Applied to Stapedotomy",*In MICCAI '01 : Proceedings of the 4th International Conference on Medical Image Computing and Computer-Assisted Intervention*, pages 1426–1429, London, UK, 2001. Springer-Verlag.

[8] C.-C. Ngan and al "Hexapod-based cochleostomyhexapod basierte cochleostomie", http://www.curac.org/curac06/download/abstracts/18.pdf.

[9] M. Leinung and al "Robotic-guided minimally-invasive cochleostomy: first results", *In: GMS Current Topics in Computer- and Robot-Assisted Surgery (GMS CURAC)*, Vol. 2, No. 1, 2007.

[10] Pierre Elbaz and al, "L'Otospongiose", Fondation Adolphe de Rothschild, Paris, 2000.

[11] Yann Nguyen and al, " Diode Laser in Otosclerosis Surgery: First Clinical Results.", Otol Neurotol. [Epub ahead of print], 28 Feb 2008, PMID: 18317398 [PubMed - as supplied by publisher].

[12] Collin ORL, Fabricant et Distributeur de matériel pour l'ORL et la Chirurgie Maxillo-Faciale, www.collin-orl.com.

[13] Daniel L. Rothbaum and al "Robot-Assisted Stapedotomy Micropick Fenestration of the Stapes Footplate", *Otolaryngology Head & Neck Surgery Journal*, 127(5), 2002, pp 417-426.

[14] K. Deb and al, "A fast and elitist multi-objective genetic algorithm : NSGA-II", *In: IEEE TRANSACTIONS ON EVOLUTIONARY COMPUTATION*, Vol. 6, No. 2, april 2002.

[15] Damien Sallé, "Conception Optimale d'Instruments Robotisés à Haute-Mobilité pour la Chirurgie Mini- Invasive", PhD thesis, Université Pierre et Marie Curie, Paris 6, 2004.